

Sensitivity of JWST to eV-Scale Decaying Axion Dark Matter

Sandip Roy^{1,*}, Carlos Blanco^{1,2,†}, Christopher Dessert^{3,‡}, Anirudh Prabhu^{4,§} and Tea Temim^{5,||}¹Department of Physics, Princeton University, Princeton, New Jersey 08544, USA²Stockholm University and The Oskar Klein Centre for Cosmoparticle Physics, Alba Nova, 10691 Stockholm, Sweden³Center for Computational Astrophysics, Flatiron Institute, New York, New York 10010, USA⁴Princeton Center for Theoretical Science, Princeton University, Princeton, New Jersey 08544, USA⁵Department of Astrophysical Sciences, Princeton University, Princeton, New Jersey 08544, USA (Received 7 December 2023; accepted 18 November 2024; published 18 February 2025)

The recently launched James Webb Space Telescope can resolve eV-scale emission lines arising from dark matter decay. We forecast the end-of-mission sensitivity to the decay of axions, a leading dark matter candidate, in the Milky Way using the blank-sky observations expected during standard operations. Searching for unassociated emission lines will constrain axions in the mass range 0.18 to 2.6 eV with axion-photon couplings $g_{a\gamma\gamma} \gtrsim 5.5 \times 10^{-12} \text{ GeV}^{-1}$. In particular, these results will constrain nucleophobic QCD axions to masses $\lesssim 0.2 \text{ eV}$.

DOI: 10.1103/PhysRevLett.134.071003

Introduction—Pseudoscalar particles with feeble couplings to photons are ubiquitous in beyond the standard model constructions and are natural dark matter (DM) candidates. A famous example is the quantum chromodynamics (QCD) axion, which was originally proposed to resolve the strong CP problem [1–7]. Similar pseudoscalar axionlike particles (ALPs) arise independently in string theory. The nondetection of weak-scale DM candidates strengthens the case that the missing $\sim 85\%$ of the matter of the Universe is composed of axions and/or ALPs. Therefore, the detection of pseudoscalars is pivotal if we hope to complete our cosmological and particle physics models of the universe. Here, we identify the recently launched James Webb Space Telescope (JWST) as a uniquely well-suited instrument to look for the astrophysical photon signatures of decaying axion and ALP DM at the eV scale.

In flavor-universal models, the QCD axion mass is constrained to be $m_a \lesssim 0.02 \text{ eV}$ by anomalous cooling bounds from neutron stars [8] and supernovae [9]. However, cooling constraints can be relaxed for axions with nucleophobic couplings, e.g., flavor-nonuniversal

scenarios [10–13], opening up the possibility of eV-scale QCD axions. Additionally, the minimal coupling of the QCD axion to gluons may lead to a hot component that can be constrained by cosmological probes, ruling out $m_a > 0.16 \text{ eV}$ [14,15]. However, these constraints are relaxed for low reheating temperatures, i.e., below the QCD scale.

Axions around the eV scale may also be produced in the correct abundance to account for DM. In the simplest scenario, misalignment production, a QCD axion with $m_a \approx \text{eV}$ can account for DM, but requires unnatural tuning of the initial misalignment angle, $|\pi - \theta_0| \lesssim e^{-1000}$ [16,17]. While there exist mechanisms that dynamically drive $|\pi - \theta_0| \rightarrow 0$ [18], such models may be ruled out by isocurvature constraints [17]. More exotic mechanisms exist to produce axions in the range $0.1 \text{ eV} \lesssim m_a \lesssim \text{eV}$. Examples of such mechanisms include unified inflaton and DM models [19,20], kinetic misalignment [21], avoided level crossing in axiverse constructions [22], and thermal production [23].

Much of the effort to detect axions in the laboratory and in astrophysical settings relies on the axion-photon interaction $\mathcal{L} \supset -g_{a\gamma\gamma} a(x) F\tilde{F}/4$, where $a(x)$ is the axion field, $g_{a\gamma\gamma} = C_{a\gamma\gamma} \alpha/2\pi f_a$ is the axion-photon coupling constant, with $C_{a\gamma\gamma}$ an $\mathcal{O}(1)$ number, F represents the electromagnetic field strength tensor, and \tilde{F} is its dual. In the mass range of interest, model-independent constraints on $g_{a\gamma\gamma}$ come from the CAST helioscope experiment [24,25] and stellar evolution in globular clusters [26]. In addition, laboratory experiments have been proposed to probe the same region of parameter space [27–29] and their projected sensitivities are displayed in Fig. 1. Another powerful technique for detecting axions is to look for their decay products. In particular, axions can decay into photons with rate $\Gamma_a = g_{a\gamma\gamma}^2 m_a^3/64\pi$ [30]. Searches for photons from

*Contact author: sandiproy@princeton.edu

†Contact author: carlosblanco2718@princeton.edu

‡Contact author: cdessert@flatironinstitute.org

§Contact author: prabhu@princeton.edu

||Contact author: temim@astro.princeton.edu

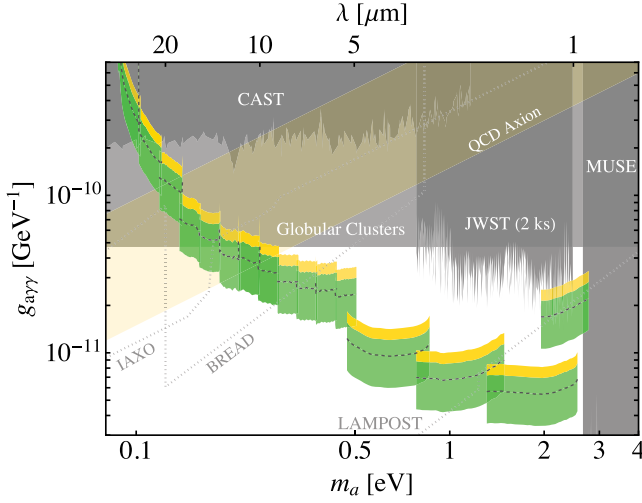


FIG. 1. The expected 95% upper limits (dotted lines) on the axion-photon coupling from an end-of-mission analysis of JWST observations. The solid green (yellow) region encloses our projections at 1(2)- σ containment. We show in solid gray the existing constraints on axions [24–26,44,45] and future experimental projections [27–29] as hatched gray lines. Possible QCD axion models live in the transparent yellow region. In order to consistently compare our projections with the recent JWST analysis [44], we rescale their constraints according to the Navarro-Frenk-White profile adopted in this Letter.

decaying axions range from radio [31] to gamma rays [32–42]. Searching for photons from decaying axion DM in the range $0.1 \text{ eV} \lesssim m_a \lesssim \text{eV}$ requires a highly sensitive infrared telescope, such as the JWST [43].

JWST represents a substantial leap in space-based imaging technology and is the scientific successor to the Hubble Space Telescope. Designed for infrared (IR) observation at the diffraction limit, JWST is capable of broad- and narrowband imagery and integral-field spectroscopy in the wavelength range of $0.6 \mu\text{m} \leq \lambda \leq 29 \mu\text{m}$, which corresponds to photon energies between about 0.05 and 2 eV [46]. JWST is equipped with instruments that are uniquely suited for the search for IR-scale decaying DM, namely, the Near-Infrared Spectrograph (NIRSpec) Integral Field Unit (IFU) [47], and the Mid-Infrared Instrument (MIRI) Medium Resolution Spectrometer (MRS) [48].

In this Letter, we show that JWST will have leading sensitivity to eV-scale axion decay at the end of mission. Because the Earth is embedded in the Milky Way (MW) DM halo, every JWST observation ever taken is sensitive to axion decay. A particularly efficient approach for DM decay searches is to analyze blank-sky observations [38,39,49], which are observations of low-surface-brightness locations in the sky. In the Mikulski Archive for Space Telescopes (MAST) database [50], we find 9.4 Ms of data usable for this purpose.

Computing the axion-decay photon flux—The expected flux density from axion decays is expressed as [51]

$$\frac{d\Phi}{d\lambda}(\lambda, l, b) = \frac{m_a}{2} \frac{\Gamma_a}{4\pi m_a} \frac{dN_\gamma(l, b)}{d\lambda} D(l, b), \quad (1)$$

where $d\Phi/d\lambda$ has units of MJy/sr Hz/ μm ; $dN_\gamma/d\lambda$ is the axion decay flux at Earth, which depends on Galactic coordinates (l, b) through Doppler broadening, shifting, and dust extinction; and the D factor $D = \int_{\text{LOS}} ds \rho_a(ds, l, b)$ is the integrated DM density along the line of sight (LOS) in units of eV/cm^2 . Often the Doppler broadening and shifting of the DM particles can be ignored, but JWST has $\mathcal{O}(0.1\%)$ energy resolution, meaning that it can resolve emission lines produced by axion decay. Furthermore, lines of sight near the Galactic plane (GP) can be attenuated due to extinction by interstellar dust [52]. Including all these effects, we have

$$\frac{dN_\gamma}{d\lambda} = \frac{m_a}{2} \frac{\int_{\text{LOS}} ds \exp(-\int_0^s ds' n_d \sigma) \rho_a(s) f[v(\lambda); r]}{\int_{\text{LOS}} ds \rho_a(s)}, \quad (2)$$

where $f[v(\lambda); r]$ is the isotropic DM velocity distribution in [49]. That velocity is a function of the observed wavelength via $|v(\lambda)| = 2/[m_a \lambda (1 - \hat{\mathbf{n}} \cdot \mathbf{v}_\odot)] - 1$, where $\hat{\mathbf{n}}$ is the direction along the line of sight and \mathbf{v}_\odot is the velocity of the Sun with respect to the Galaxy [53,54]. The extinction is provided by the exponential factor, where $n_d(s, l, b)$ is the dust density and $\sigma(\lambda)$ is its cross section with photons. Although some three-dimensional models of the Galactic dust distribution exist [55], they are typically not reliable out to distances of order the Milky Way scale radius, so in this Letter we conservatively model the extinction as if all emission originated at infinity, so that $\exp(-\int_0^s ds' n_d \sigma) \rightarrow 10^{-0.44A_\lambda}$, where A_λ is the Galactic extinction at wavelength λ . We use the Galactic dust models in [56,57] and the extinction curve from [58] to compute the Galactic extinction [for details, see Supplemental Material (SM) [59]]. The axion decays to a diphoton final state, meaning that $\int d\lambda dN_\gamma/d\lambda = 2 \times 10^{-0.44A_\lambda/m_a}$ and the total expected flux simplifies to $\Phi = \Gamma_a D_{\text{eff}}/4\pi$, where D_{eff} is the D factor times the attenuation due to dust. We compute the D factor in the Milky Way using a Navarro-Frenk-White profile [60,61] with DM density at Earth $\rho_{\text{Earth}} = 0.29 \text{ GeV}/\text{cm}^3$ and a scale radius $r_s = 19.1 \text{ kpc}$, using recent results calibrated on Gaia DR2 data [62], along with a Galactic Center-Earth distance $d_{\text{Earth}} = 8.23 \text{ kpc}$ [63]. Using different DM profiles such as those in [64,65] does not change our final projections significantly (see SM for details). D_{eff} at $1 \mu\text{m}$ (i.e., $m_a = 2.5 \text{ eV}$) is shown in Fig. 2. With knowledge of the astrophysical parameters, the axion DM decay flux is given by [37]

$$\Phi(l, b) = 1.0 \times 10^{-9} \text{ erg}/\text{cm}^2/\text{s}/\text{sr} \left(\frac{g_{\gamma\gamma}}{10^{-11} \text{ GeV}^{-1}} \right)^2 \times \left(\frac{m_a}{1 \text{ eV}} \right)^3 \left(\frac{D_{\text{eff}}}{10^{31} \text{ eV}/\text{cm}^2} \right), \quad (3)$$

where the line wavelength $\lambda = 2.5(1 \text{ eV}/m_a) \mu\text{m}$, corresponding to an energy $E_\gamma = m_a/2$. In particular, the MIRI

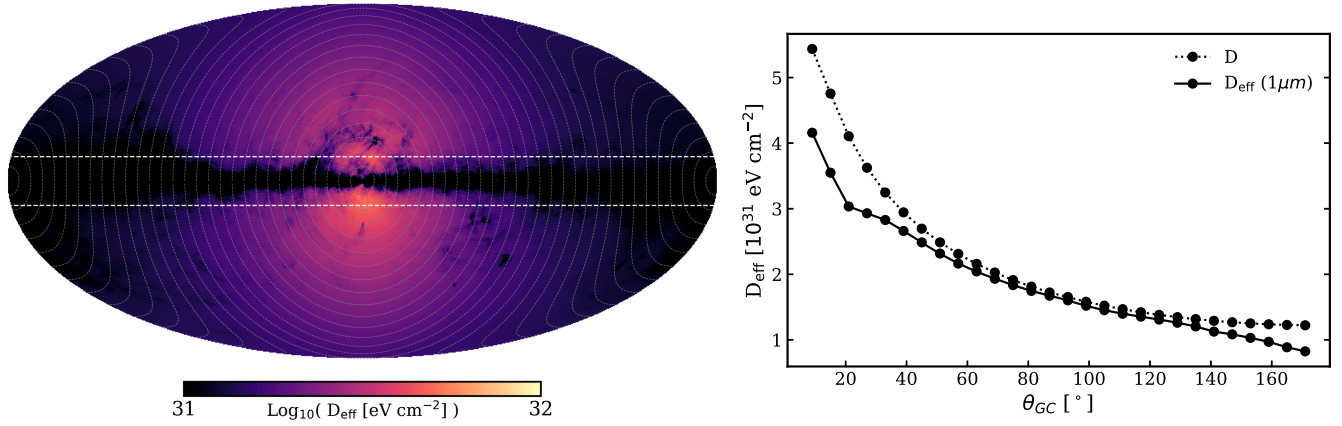


FIG. 2. Left panel: D_{eff} in Galactic coordinates at $1\mu\text{m}$, corresponding to $m_a = 2.5\text{ eV}$. The gray dashed lines delineate our ring edges and the dashed white lines are $|b| = 10^\circ$, below which we mask out in our analysis. Right panel: angular-averaged D_{eff} at a wavelength of $1\mu\text{m}$ (solid line) and without any dust extinction (dotted line), avoiding the masked Galactic plane region. Lines of sight close to the Galactic plane at $\theta_{\text{GC}} = 0^\circ$ and $\theta_{\text{GC}} = 180^\circ$ experience the strongest dust extinction. At wavelengths greater than $1\mu\text{m}$, the dust extinction decreases as shown in detail in the SM.

MRS filters are sensitive to axions with masses $0.089\text{ eV} \leq m_a \leq 0.506\text{ eV}$, while the NIRSpec IFU filters are sensitive to $0.47\text{ eV} \leq m_a \leq 2.75\text{ eV}$, so that our projections cover unexplored parameter space over an order of magnitude in axion mass.

In this Letter, we compute the expected sensitivity of JWST to axion decays in the Milky Way halo. To this end we need to know the total exposure time usable for blank-sky observations. Every IFU observation taken is useful, unless the source is sufficiently extended such that emission will dominate the observation. On the other hand, point sources can be removed via a spatial mask. JWST’s lifetime is fuel-limited, and the telescope was designed to operate for 10 yr, but is expected to continue operating for about 20 yr. Not all of this time will be spent observing the blank sky; in particular, the observing efficiency is expected to be around 70% [66]. We pay an additional penalty because only some fraction of this time will be spent observing with the IFU modes. We compute the expected exposure time in each instrument mode in a data-driven way by extrapolating the first ~ 1.5 yr of observations, taken between March 17, 2022, and November 6, 2023, to that expected in 10 yr of operation. We obtain the exposure times from the MAST database. In this

computation we exclude observations with extended sources and observations within the GP mask, which collectively account for approximately 30% of the total exposure time. However, we note that extended source observations are typically accompanied by dedicated background observations, so that this approach is extremely conservative. Our expected exposure times are shown in Table I. Given that the JWST IFU field of view (FOV), $\mathcal{O}(10\text{ arcsec}^2)$ depending on the observing mode, is only 1 part in 10^{11} of the full sky at any time, we need to know the observing pattern. We assume that JWST observes isotropically across the full sky. In the SM, we show results where we instead assume the end-of-mission exposure time distribution is given by that derived from completed observations to date in the MAST database, which does not appreciably alter the results.

We use the JWST_BACKGROUND [67] tool developed by JWST to compute the background contribution at a given point on the sky. The astrophysical background is modeled with four components. The dominant contributions are the in-field zodiacal light [68–70] and the in-field interstellar medium emission [56]. Zodiacal emission arises through the reflection of sunlight by dust in our Solar System and thus dominates the background at low ecliptic latitudes.

TABLE I. The exposure times t_{exp} in Ms for MIRI and ks for NIRSpec assumed in our projections for each observing mode.

		MIRI MRS Grating			Short	Medium	Long		
		t_{exp} (Ms)			12.5	12.4	12.5		
NIRSpec Filter	F070LP	F100LP	F170LP	F290LP	F070LP	F100LP	F170LP	F290LP	
	G140M	G140M	G235M	G395M	G140H	G140H	G235H	G395H	
t_{exp} (ks)	1.4	750	1060	1980	5.9	1300	6900	8070	

The interstellar medium background is produced by dust emission within the Milky Way and thus dominates at low Galactic latitudes. Other background components include the astrophysical and detector stray light [71,72] and the thermal self-emission that dominate at wavelengths $\gtrsim 20 \mu\text{m}$. For further details and a measurement of the astrophysical background, see Ref. [73].

Projecting JWST's sensitivity to axion decays—Using the procedure developed in Ref. [39], we bin the data in 30 concentric rings around the Galactic Center (GC) of width 6° and mask the GP up to $b \leq 10^\circ$ so that the innermost and outermost rings are entirely masked. This mask is motivated by the fact that the dust extinction can be difficult to calculate in the GP due to a larger variety of dust molecules [58], and we wish to remain insensitive to such details. As we show in the SM, smaller masks actually reduce D_{eff} near the GP, although we would gain $\sim 10\%$ in exposure time. We compute the expected exposure time in each JWST spectroscopic mode and ring. Note that there are 12 MRS modes, but they are split into groups of three by wavelength, and the entire group is observed simultaneously. There are eight NIRSpec filters over four wavelength bands. Each band is observed in high and medium resolution. We do not consider the NIRSpec PRISM mode, which has reduced spectral resolution.

The axion decay flux is modeled as in Eq. (1), where D_{eff} is computed by averaging over each ring. In the course of this averaging, the line is broadened beyond the intrinsic width of 220 km/s of Doppler broadening because the Doppler shifting can change significantly over a ring. We could shift the data to the Galactic rest frame, but this introduces difficult-to-model bin-to-bin correlations in the data [74]. We compute the root-mean-square Doppler shift in each ring and add it in quadrature to the Doppler broadening to determine the observed width of the line v_{line} . For the innermost ring, nearly transverse to the Solar motion, the width is 220 km/s; for the rings 90° from the GC the width increases to ~ 275 km/s, (for details, see SM).

To model the expected signal-to-noise ratio (SNR) for the axion decay, we use the output of the JWST Exposure Time Calculator (ETC) [75] in each analysis ring assuming a fixed exposure time t_{exp} and axion-photon coupling $g_{a\gamma\gamma}$. This approach is agnostic to any particular analysis strategy, such as parametric likelihood-based frequentist modeling as in Ref. [38] or nonparametric approaches such as Gaussian processes as in [39,76], which should be developed when performing analysis on real data. However, we verified on simulated data that the parametric approach, where, e.g., the signal line is modeled along with a quadratic background model, returns results consistent with that of the ETC. Note, however, that we have not included possible systematics into this projection. For instance, we do not account for diffuse astrophysical line emission. In the vicinity of bright astrophysical lines, our limits may disappear; however, these lines exist over only a

small fraction of the parameter space. There are known possible spurious line signals [66]: scattered light from a bright line emitters and the $12.2 \mu\text{m}$ MRS spectral leak. The former should affect only a few individual observations, and particular wavelengths with less-understood instrumental spectral features can be avoided, so we expect these issues to have minimal impact on our results.

The ETC incorporates sky-dependent background models; we query the background model at the point in the ring closest to the ecliptic plane where the backgrounds are largest outside $|b| \leq 10^\circ$. We show the effects of other choices in the SM. We query the ETC for each observing mode at an axion mass such that the decay occurs in the mode's wavelength range. The axion signal in each ring is input as a spectral line positioned at a frequency $m_a/2$ with the observed ring-dependent width. We use the scaling relation in Eq. (4), verified empirically with the JWST ETC, to determine the SNR across the entire filter bandwidth and repeat this process for each NIRSpec and MIRI filter of interest (where the N_a and N_{bkg} represent the detector counts for axions and background, respectively, ϵ_λ represents the wavelength-dependent filter throughput, and $\Phi_{\text{bkg},\lambda}$ represents the wavelength and line-of-sight-dependent background and instrumental noise flux). We then compute Asimov likelihoods [77] in each ring and filter and multiply the likelihoods in each ring to obtain a joint likelihood. For each value of m_a , we solve for the 95% upper limit on the axion-photon coupling strength $g_{a\gamma\gamma}^{95}$ such that $\text{SNR}|_{\lambda=2/m_a} = \sqrt{2.71}$, given that Wilks' theorem holds,

$$\text{SNR}(\lambda) = \frac{N_a}{\sqrt{N_{\text{bkg}}}} \propto m_a^3 g_{a\gamma\gamma}^2 D_{\text{eff}}^{\frac{1}{2}} t_{\text{exp}}^{\frac{1}{2}} \epsilon_\lambda^{\frac{1}{2}} \Phi_{\text{bkg},\lambda}^{-\frac{1}{2}}. \quad (4)$$

We present our projected 95% upper limits in Fig. 1, along with their 1- and 2- σ enclosing regions. In particular, we show that JWST will have leading sensitivity to axions over an order of magnitude in mass $0.18 \text{ eV} \leq m_a \leq 2.6 \text{ eV}$. The NIRSpec IFU filters, covering axion masses between $0.5 \text{ eV} \leq m_a \leq 2.6 \text{ eV}$, reach axion-photon couplings down to $5.5 \times 10^{-12} \text{ GeV}^{-1}$. We show our MIRI MRS projections in the 12 bands at smaller masses, which are somewhat weaker, although they promise to probe nucleophobic QCD axion scenarios down to 0.18 eV. Our analysis shows that JWST has the ability to rule out a QCD axion DM candidate above about 0.2 eV, whether or not it is coupled to baryonic matter, making this analysis particularly complementary to other astrophysical probes.

Discussion and conclusion—JWST is the first telescope with exquisite enough sensitivity to near- and mid-IR emission lines to probe viable axion DM. Although JWST was not designed with axion decay searches in mind, it is nevertheless a powerful tool in the search for axions owing to its spectral resolution, which is precise enough to resolve lines resulting from DM decay. In this

Letter, we show that an analysis of the end-of-mission blank-sky observations will cover novel axion parameter space in a region that is currently unexplored by terrestrial experiments. This will effectively rule out a QCD axion DM candidate heavier than about 0.2 eV, regardless of its matter couplings. Importantly, the blank-sky observations discussed in this Letter will be made in the course of the normal operations of JWST, and require no changes in the observing strategy.

Another search strategy could be to observe a dwarf galaxy such as Draco dSph. Typically the blank-sky strategy is stronger, but the JWST FOV is significantly smaller than most telescopes used to search for DM decay, while the dwarf D factors increase when averaged over smaller FOVs around their centers. Furthermore, dust extinction reduces the MW D factor while it is irrelevant for dwarfs not in the plane of the Galaxy. Accounting for these effects, Draco hosts a larger D factor than any MW location, which we estimate to be $\sim(9 \pm 2.5) \times 10^{31}$ eV/cm² in the JWST FOV (the variation with observing mode is small) [78], which is conservatively about 3 times as large as the MW average. The typical dwarf velocity dispersion is also smaller than the MW, $\mathcal{O}(10^{-4})$ [79], which means that DM decay lines originating in dwarfs would be unresolved by JWST, but this has a relatively minor effect on our sensitivity. Draco and other dwarfs have not to date been observed by JWST except in imaging modes, and are unlikely to be observed in normal operations. A typical single-target observation could achieve total exposure times of around 100 ks, about 200 times smaller than that of our combined exposure. Therefore, such an analysis could not exceed the sensitivity of an end-of-mission blank-sky analysis (except in the mass range from 2.55 to 2.66 eV, which is probed only by the low-exposure F070LP filters). For example, assuming a 100 ks observation of Draco across the four high-resolution NIRSpec modes, we estimate a peak sensitivity of $g_{\text{arr}}^{95} \approx 8 \times 10^{-12}$ GeV⁻¹. However, a 100 ks dwarf observation in one particular filter would result in sensitivity over a smaller mass range, which is competitive with that forecasted here.

In this Letter, we focus on forecasting the JWST end-of-mission sensitivity to axion decay. JWST has now been in operation for ~ 1.5 yr, and therefore has collected 15% of its total data. An analysis of only the currently available data would still provide leading sensitivity, but weaker than that projected here by a factor of $0.15^{-1/4} \sim 1.6$, which we leave to future work.

This research made extensive use of the publicly available codes `ASTROPY` [80–82], `DUST_EXTINCTION` [83], `DUSTMAPS` [55], `HEALPIX` [84], `HEALPY` [85], `IPYTHON` [86], `JUPYTER` [87], `MATHEMATICA` [88], `MATPLOTLIB` [89], `NUMPY` [90], `PYTHON` [91] `SCIPY` [92], and `UNYT` [93].

Note added—Recently, Ref. [44] appeared on the arXiv, also studying Milky Way axion decay signatures using JWST. Our works have some overlap but are complementary; the main result of that work is the analysis of two NIRSpec observations. While that work projects the end-of-mission sensitivity for two NIRSpec filters through extrapolation of their limits, we take into account spatial information in both the decay signal and the astrophysical backgrounds to project sensitivity for all JWST IFU detectors. We note that we find that our NIRSpec projections are weaker by a factor of ~ 2 .

Acknowledgments—We thank Dylan Folsom, Joshua Foster, Mariia Khelashvili, Mariangela Lisanti, Hongwan Liu, Benjamin Safdi, and the JWST Space Telescope Science Institute help staff. A.P. acknowledges support from the Princeton Center for Theoretical Science post-doctoral fellowship. The work of C.B. was supported in part by NASA through the NASA Hubble Fellowship Program Grant No. HST-HF2-51451.001-A awarded by the Space Telescope Science Institute, which is operated by the Association of Universities for Research in Astronomy, Inc., for NASA, under Contract No. NAS5-26555. Part of this work was done at the Aspen Center for Physics, which is supported by National Science Foundation Grant No. PHY-1607611. S.R. was supported by the Department of Energy (DOE) under Award No. DE-SC0007968.

-
- [1] R. D. Peccei and H. R. Quinn, *Phys. Rev. D* **16**, 1791 (1977).
 - [2] R. D. Peccei and H. R. Quinn, *Phys. Rev. Lett.* **38**, 1440 (1977).
 - [3] S. Weinberg, *Phys. Rev. Lett.* **40**, 223 (1978).
 - [4] F. Wilczek, *Phys. Rev. Lett.* **40**, 279 (1978).
 - [5] J. Preskill, M. B. Wise, and F. Wilczek, *Phys. Lett.* **120B**, 127 (1983).
 - [6] L. F. Abbott and P. Sikivie, *Phys. Lett.* **120B**, 133 (1983).
 - [7] M. Dine and W. Fischler, *Phys. Lett.* **120B**, 137 (1983).
 - [8] M. Buschmann, C. Dessert, J. W. Foster, A. J. Long, and B. R. Safdi, *Phys. Rev. Lett.* **128**, 091102 (2022).
 - [9] A. Lella, P. Carezza, G. Co', G. Lucente, M. Giannotti, A. Mirizzi, and T. Rauscher, [arXiv:2306.01048](https://arxiv.org/abs/2306.01048).
 - [10] L. Di Luzio, F. Mescia, E. Nardi, P. Panci, and R. Ziegler, *Phys. Rev. Lett.* **120**, 261803 (2018).
 - [11] F. Björkeröth, L. Di Luzio, F. Mescia, and E. Nardi, *J. High Energy Phys.* **02** (2019) 133.
 - [12] M. Badziak and K. Harigaya, *J. High Energy Phys.* **06** (2023) 014.
 - [13] F. Takahashi and W. Yin, [arXiv:2301.10757](https://arxiv.org/abs/2301.10757).
 - [14] A. Notari, F. Rompineve, and G. Villadoro, *Phys. Rev. Lett.* **131**, 011004 (2023).
 - [15] F. Bianchini, G. G. di Cortona, and M. Valli, [arXiv:2310.08169](https://arxiv.org/abs/2310.08169).
 - [16] D. J. Marsh, *Phys. Rep.* **643**, 1 (2016).
 - [17] A. Arvanitaki, S. Dimopoulos, M. Galanis, L. Lehner, J. O. Thompson, and K. Van Tilburg, *Phys. Rev. D* **101**, 083014 (2020).

- [18] F. Takahashi and W. Yin, *J. High Energy Phys.* **10** (2019) 120.
- [19] R. Daido, F. Takahashi, and W. Yin, *J. High Energy Phys.* **02** (2018) 104.
- [20] R. Daido, F. Takahashi, and W. Yin, *J. Cosmol. Astropart. Phys.* **05** (2017) 044.
- [21] R. T. Co, L. J. Hall, and K. Harigaya, *Phys. Rev. Lett.* **124**, 251802 (2020).
- [22] D. Cyncynates and J. O. Thompson, [arXiv:2306.04678](https://arxiv.org/abs/2306.04678).
- [23] W. Yin, *J. High Energy Phys.* **05** (2023) 180.
- [24] E. Arik *et al.* (CAST Collaboration), *J. Cosmol. Astropart. Phys.* **02** (2009) 008.
- [25] M. Arik *et al.* (CAST Collaboration), *Phys. Rev. Lett.* **112**, 091302 (2014).
- [26] M. J. Dolan, F. J. Hiskens, and R. R. Volkas, *J. Cosmol. Astropart. Phys.* **10** (2022) 096.
- [27] E. Armengaud *et al.* (IAXO Collaboration), *J. Cosmol. Astropart. Phys.* **06** (2019) 047.
- [28] J. Liu *et al.*, *Phys. Rev. Lett.* **128**, 131801 (2022).
- [29] M. Baryakhtar, J. Huang, and R. Lasenby, *Phys. Rev. D* **98**, 035006 (2018).
- [30] R. M. Barnett *et al.* (Particle Data Group), *Phys. Rev. D* **54**, 1 (1996).
- [31] At low frequency the decay rate is Bose-enhanced relative to the previously-quoted vacuum decay rate.
- [32] A. Caputo, M. Regis, M. Taoso, and S. J. Witte, *J. Cosmol. Astropart. Phys.* **03** (2019) 027.
- [33] M. H. Chan, *Sci. Rep.* **11**, 20087 (2021).
- [34] Y. Sun, K. Schutz, A. Nambrath, C. Leung, and K. Masui, *Phys. Rev. D* **105**, 063007 (2022).
- [35] M. A. Buen-Abad, J. Fan, and C. Sun, *Phys. Rev. D* **105**, 075006 (2022).
- [36] Y. Sun, K. Schutz, H. Sewalls, C. Leung, and K. W. Masui, *Phys. Rev. D* **109**, 043042 (2024).
- [37] D. Grin, G. Covone, J.-P. Kneib, M. Kamionkowski, A. Blain, and E. Jullo, *Phys. Rev. D* **75**, 105018 (2007).
- [38] C. Dessert, N. L. Rodd, and B. R. Safdi, *Science* **367**, 1465 (2020).
- [39] J. W. Foster, M. Kongsore, C. Dessert, Y. Park, N. L. Rodd, K. Cranmer, and B. R. Safdi, *Phys. Rev. Lett.* **127**, 051101 (2021).
- [40] F. Calore, A. Dekker, P. D. Serpico, and T. Siebert, *Mon. Not. R. Astron. Soc.* **520**, 4167 (2023).
- [41] W. DeRocco, S. Wegsman, B. Grefenstette, J. Huang, and K. Van Tilburg, *Phys. Rev. Lett.* **129**, 101101 (2022).
- [42] C. Blanco and D. Hooper, *J. Cosmol. Astropart. Phys.* **03** (2019) 019.
- [43] T. Bessho, Y. Ikeda, and W. Yin, *Phys. Rev. D* **106**, 095025 (2022).
- [44] R. Janish and E. Pinetti, preceding Letter, *Phys. Rev. Lett.* **134**, 071002 (2025).
- [45] E. Todarello, M. Regis, J. Reynoso-Cordova, M. Taoso, D. Vaz, J. Brinchmann, M. Steinmetz, and S. L. Zoutendijk, [arXiv:2307.07403](https://arxiv.org/abs/2307.07403).
- [46] M. Greenhouse, in *2019 IEEE Aerospace Conference, Big Sky, MT, USA* (IEEE, 2019), pp. 1–13, [10.1109/AERO.2019.8742209](https://doi.org/10.1109/AERO.2019.8742209).
- [47] P. Jakobsen *et al.*, *Astron. Astrophys.* **661**, A80 (2022).
- [48] M. Wells *et al.*, *Publ. Astron. Soc. Pac.* **127**, 646 (2015).
- [49] C. Dessert, O. Ning, N. L. Rodd, and B. R. Safdi, [arXiv:2305.17160](https://arxiv.org/abs/2305.17160).
- [50] MAST 2021, MAST Portal Guide, edited by R. A. Shaw, B. Cherinka, and P. Forshay (Version 2; Baltimore: STScI), <https://outerspace.stsci.edu/display/MASTDOCS/Portal+Guide>.
- [51] M. Lisanti, S. Mishra-Sharma, N. L. Rodd, B. R. Safdi, and R. H. Wechsler, *Phys. Rev. D* **97**, 063005 (2018).
- [52] B. T. Draine, *Annu. Rev. Astron. Astrophys.* **41**, 241 (2003).
- [53] F. Mignard, *Astron. Astrophys.* **354**, 522 (2000), <https://ui.adsabs.harvard.edu/abs/2000A%26A...354..522M/abstract>.
- [54] R. Schönrich, J. Binney, and W. Dehnen, *Mon. Not. R. Astron. Soc.* **403**, 1829 (2010).
- [55] G. M. Green, E. Schlafly, C. Zucker, J. S. Speagle, and D. Finkbeiner, *Astrophys. J.* **887**, 93 (2019).
- [56] D. J. Schlegel, D. P. Finkbeiner, and M. Davis, *Astrophys. J.* **500**, 525 (1998).
- [57] E. F. Schlafly and D. P. Finkbeiner, *Astrophys. J.* **737**, 103 (2011).
- [58] J. Gao, A. Li, and B. W. Jiang, *Earth Planets Space* **65**, 1127 (2013).
- [59] See Supplemental Material at <http://link.aps.org/supplemental/10.1103/PhysRevLett.134.071003> for a discussion of the spectrospatial properties of the decay signal, the astrophysical backgrounds, and the impact of extinction of the decay signal due to Galactic dust.
- [60] J. F. Navarro, C. S. Frenk, and S. D. M. White, *Astrophys. J.* **462**, 563 (1996).
- [61] J. F. Navarro, C. S. Frenk, and S. D. M. White, *Astrophys. J.* **490**, 493 (1997).
- [62] M. Cautun, A. Benítez-Llambay, A. J. Deason, C. S. Frenk, A. Fattahi, F. A. Gómez, R. J. J. Grand, K. A. Oman, J. F. Navarro, and C. M. Simpson, *Mon. Not. R. Astron. Soc.* **494**, 4291 (2020).
- [63] H. W. Leung, J. Bovy, J. T. Mackereth, J. A. S. Hunt, R. R. Lane, and J. C. Wilson, *Mon. Not. R. Astron. Soc.* **519**, 948 (2022).
- [64] X. Ou, A.-C. Eilers, L. Necib, and A. Frebel, *Mon. Not. R. Astron. Soc.* **528**, 693 (2024).
- [65] K. A. Oman and A. H. Riley, *Mon. Not. R. Astron. Soc.: Letters* **532**, L48 (2024).
- [66] Jwst user documentation, <https://jwst-docs.stsci.edu/>.
- [67] <https://jwst-docs.stsci.edu/jwst-other-tools/jwst-backgrounds-tool>
- [68] T. Kelsall, J. L. Weiland, B. A. Franz, W. T. Reach, R. G. Arendt, E. Dwek, H. T. Freudenreich, M. G. Hauser, S. H. Moseley, N. P. Odegard, R. F. Silverberg, and E. L. Wright, *Astrophys. J.* **508**, 44 (1998).
- [69] E. L. Wright, *Astrophys. J.* **496**, 1 (1998).
- [70] V. Gorjian, E. L. Wright, and R. R. Chary, *Astrophys. J.* **536**, 550 (2000).
- [71] P. A. Lightsey, *SPIE* **9904**, 99040A (2016).
- [72] R. J. Wainscoat, M. Cohen, K. Volk, H. J. Walker, D. E. Schwartz, R. J. Wainscoat, M. Cohen, K. Volk, H. J. Walker, and D. E. Schwartz, *Astrophys. J. Suppl. Ser.* **83**, 111 (1992).
- [73] J. R. Rigby *et al.*, *Publ. Astron. Soc. Pac.* **135**, 048002 (2023).
- [74] C. Dessert, J. W. Foster, Y. Park, and B. R. Safdi, [arXiv:2309.03254](https://arxiv.org/abs/2309.03254).

- [75] Jwst exposure time calculator, <https://jwst.etc.stsci.edu/>.
- [76] M. Frate, K. Cranmer, S. Kalia, A. Vandenberg-Rodes, and D. Whiteson, [arXiv:1709.05681](https://arxiv.org/abs/1709.05681).
- [77] G. Cowan, K. Cranmer, E. Gross, and O. Vitells, *Eur. Phys. J. C* **71**, 1554 (2011); **73**, 2501(E) (2013).
- [78] N. W. Evans, J. L. Sanders, and A. Geringer-Sameth, *Phys. Rev. D* **93**, 103512 (2016).
- [79] A. W. McConnachie, *Astron. J.* **144**, 4 (2012).
- [80] Astropy Collaboration, *Astron. Astrophys.* **558**, A33 (2013).
- [81] Astropy Collaboration, *Astron. J.* **156**, 123 (2018).
- [82] Astropy Collaboration, *Astrophys. J.* **935**, 167 (2022).
- [83] K. Gordon, dust_extinction: A PYTHON package for interstellar dust extinction laws and curves, Available at https://github.com/karllark/dust_extinction (2023) (accessed: October 2023).
- [84] K. M. Górski, E. Hivon, A. J. Banday, B. D. Wandelt, F. K. Hansen, M. Reinecke, and M. Bartelmann, *Astrophys. J.* **622**, 759 (2005).
- [85] A. Zonca, L. Singer, D. Lenz, M. Reinecke, C. Rosset, E. Hivon, and K. Gorski, *J. Open Source Software* **4**, 1298 (2019).
- [86] F. Pérez and B. E. Granger, *Comput. Sci. Eng.* **9**, 21 (2007).
- [87] T. Kluyver *et al.*, *Positioning and Power in Academic Publishing: Players, Agents and Agendas—Proceedings of the 20th International Conference on Electronic Publishing, ELPUB 2016* (2016), 87, 10.3233/978-1-61499-649-1-87.
- [88] W. R. Inc., MATHEMATICA, Version 13.3, Champaign, IL, 2023.
- [89] J. D. Hunter, *Comput. Sci. Eng.* **9**, 90 (2007).
- [90] C. R. Harris *et al.*, *Nature (London)* **585**, 357 (2020).
- [91] G. Van Rossum and F. L. Drake, *PYTHON3 Reference Manual* (CreateSpace, Scotts Valley, CA, 2009).
- [92] P. Virtanen *et al.*, *Nat. Methods* **17**, 261 (2020).
- [93] N. J. Goldbaum, J. A. ZuHone, M. J. Turk, K. Kowalik, and A. L. Rosen, *J. Open Source Software* **3**, 809 (2018).